

# Mutual information between in- and output trajectories of biochemical networks

Filipe Tostevin and Pieter Rein ten Wolde  
*FOM Institute for Atomic and Molecular Physics,  
Kruislaan 407, 1098 SJ Amsterdam, The Netherlands.*  
(Dated: December 29, 2008)

Biochemical networks can respond to temporal characteristics of time-varying signals. To understand how reliably biochemical networks can transmit information we must consider how an input signal as a function of time—the input trajectory—can be mapped onto an output trajectory. Here we estimate the mutual information between in- and output trajectories using a Gaussian model. We study how reliably the chemotaxis network of *E. coli* can transmit information on the ligand concentration to the flagellar motor, and find the input power spectrum that maximizes the information transmission rate.

Cells continually have to respond to a wide range of intra- and extracellular signals. These signals have to be detected, encoded, transmitted and decoded by biochemical networks. In the absence of biochemical noise, a particular input signal will lead to a unique output signal, allowing the cell to respond appropriately. Recent experiments, however, have vividly demonstrated that biochemical networks can be highly stochastic [1], and a key question is therefore how reliably biochemical networks can transmit information in the presence of noise.

To address this question, we must recognize that the message may be contained in the *temporal dynamics* of the input signal. A well-known example is bacterial chemotaxis, where the concentration of the intracellular messenger protein depends not on the current ligand concentration, but rather on whether this concentration has changed in the recent past [2]—the response of the network thus depends on the *history* of the input signal. Moreover, the input signal may be encoded into the temporal dynamics of the signal transduction pathway. For example, stimulation of the rat PC-12 system with a neuronal growth factor gives rise to a sustained response of the Raf-Mek-Erk pathway, while stimulation with an epidermal growth factor leads to a transient response [3]. In all these cases, the message is encoded not in the concentration of some chemical species at a specific moment in time, but rather in its concentration as a function of time. Importantly, whether the network that processes the signal can reliably respond to it, depends not only on the instantaneous value of the signal, but also on the time scale over which it changes. In general, the in- and output signals of biochemical networks are time-continuous signals with non-zero correlations times. To understand how reliably biochemical networks can transmit information, we need to know how accurately an input signal as a function of time—the input *trajectory*—can be mapped onto an output trajectory. In this article, we take an information theoretic approach to this question.

A natural measure for the quality of information transmission is the mutual information between the input signal  $I$  and the network response  $O$ , given by [4]

$$M(I, O) = H(O) - H(O|I). \quad (1)$$

Here,  $H(O) \equiv - \int dO p(O) \log p(O)$ , with  $p(O)$  the probability distribution of  $O$ , is the information entropy of the output  $O$ ;  $H(O|I) \equiv - \int dI p(I) \int dO p(O|I) \log p(O|I)$  is the average (over inputs  $I$ ) information entropy of  $O$  given  $I$ , with  $p(O|I)$  the conditional probability distribution of  $O$  given  $I$ . Recently, the mutual information between the *instantaneous* values of the in- and output signals of biochemical networks has been investigated [5, 6], although in these studies the temporal correlations in the input signals were ignored. Here we investigate the mutual information between in- and output trajectories.

*Mutual information between trajectories*—We consider a biochemical network in steady state with one input species  $S$  with copy number  $S$  and one output species  $X$  with copy number  $X$ . The mutual information between in- and output trajectories is found by taking the possible input and output signals  $I$  and  $O$  in Eq. 1 to be the possible trajectories  $S(t)$  and  $X(t)$ :

$$M(S, X) = \int \mathcal{D}S(t) \int \mathcal{D}X(t) p(S(t), X(t)) \log \frac{p(S(t), X(t))}{p(S(t))p(X(t))}. \quad (2)$$

Calculating the mutual information between in- and output trajectories is, in general, a formidable task, given the high-dimensionality of the trajectory space. However, for a Gaussian model, which we will use here, the mutual information can be obtained analytically. In such a Gaussian model it is assumed that the system is in steady-state, that variations in the input signal obey Gaussian statistics, and that fluctuations in the copy numbers of the processing network are small, such that the coupling between them can be linearized and the linear-noise approximation can be used [7]. Recent modelling studies have shown that the noise properties of a large class of biochemical networks are well described by such a Gaussian model, even when the copy numbers are as low as ten [6, 8]. Importantly, it can be shown that when the protein numbers do not obey Gaussian statistics, the mutual information calculated in the Gaussian approximation provides a lower bound on the channel capacity of the full system [9].

In the Gaussian model, the statistics of the in- and

output signals is given by

$$p(\mathbf{v}) = \frac{1}{(2\pi)^N |\mathbf{Z}|^{1/2}} \exp\left(-\frac{1}{2} \mathbf{v}^T \mathbf{Z}^{-1} \mathbf{v}\right). \quad (3)$$

Here, the vector  $\mathbf{v} \equiv (\mathbf{s}, \mathbf{x})$ , with  $\mathbf{s} = (s(t_1), s(t_2), \dots, s(t_N))$  constructed from the input signal sampled at times  $t = t_1, \dots, t_N$ , and  $\mathbf{x} = (x(t_1), x(t_2), \dots, x(t_N))$ ;  $s(t)$  and  $x(t)$  are the deviations of  $S$  and  $X$  away from their steady-state values,  $\langle S \rangle$  and  $\langle X \rangle$ , respectively. The  $2N \times 2N$  covariance matrix  $\mathbf{Z}$  has the form

$$\mathbf{Z} = \begin{pmatrix} \mathbf{C}^{ss} & \mathbf{C}^{xs} \\ \mathbf{C}^{sx} & \mathbf{C}^{xx} \end{pmatrix}, \quad (4)$$

where  $\mathbf{C}^{\alpha\beta}$  is an  $N \times N$  matrix with elements

$$\mathbf{C}_{ij}^{\alpha\beta} = C_{\alpha\beta}(t_i - t_j) = \langle \alpha(t_i) \beta(t_j) \rangle. \quad (5)$$

In the limit that the in- and output signals are time-continuous, the mutual information rate between the in- and output trajectories is given by [10]

$$R(\mathbf{s}, \mathbf{x}) = \lim_{T \rightarrow \infty} M(\mathbf{s}, \mathbf{x})/T \quad (6)$$

$$= -\frac{1}{4\pi} \int_{-\infty}^{\infty} d\omega \ln \left[ 1 - \frac{|S_{SX}(\omega)|^2}{S_{SS}(\omega) S_{XX}(\omega)} \right], \quad (7)$$

where the power spectrum  $S_{\alpha\beta}(\omega)$  is the Fourier transform of  $C_{\alpha\beta}(t - t')$ .

A biochemical network differs from a channel in telecommunication or electronics, in that the reaction that detects the input signal can introduce correlations between the signal and the intrinsic noise of the reactions that constitute the processing network [8]; these correlations are a consequence of the molecular character of the components and thus unique to (bio)chemical systems. If the detection reaction does not introduce correlations, then the power spectrum of the output signal,  $S_{XX}(\omega)$ , is given by the spectral addition rule [8]:

$$S_{XX}(\omega) = N(\omega) + g^2(\omega) S_{SS}(\omega). \quad (8)$$

Here,  $N(\omega)$  is the intrinsic noise of the processing network,  $S_{SS}(\omega)$  is the power spectrum of the input signal, and  $g^2(\omega) = |S_{SX}(\omega)|^2 / S_{SS}(\omega)^2$  is the frequency-dependent gain. Identifying the spectrum of the transmitted signal to be  $P(\omega) = g^2(\omega) S_{SS}(\omega)$ , Eq. 7 can be rewritten as

$$R(\mathbf{s}, \mathbf{x}) = \frac{1}{4\pi} \int_{-\infty}^{\infty} d\omega \ln(1 + P(\omega)/N(\omega)), \quad (9)$$

a well-known result for a time-continuous Gaussian channel [11]. When the detection reaction does introduce correlations between variations in the input signal and the noise of the processing network, one can still define  $g^2(\omega)$  and  $P(\omega)$  as above and apply Eq. 9. However, in this

case  $N(\omega)$  and  $g^2(\omega)$  are not properties intrinsic to the processing network, but also depend on the statistics of the input signal.

The Gaussian model described above can also be used to calculate the mutual information between instantaneous values of  $s$  and  $x$ ,

$$M^{\text{ins}}(s, x) = -\frac{1}{2} \ln \left( 1 - \frac{\sigma_{SX}^4}{\sigma_{SS}^2 \sigma_{XX}^2} \right), \quad (10)$$

where  $\sigma_{SS}^2 = \langle s^2 \rangle$ ,  $\sigma_{XX}^2 = \langle x^2 \rangle$ , and  $\sigma_{SX}^2 = \langle sx \rangle$ . The instantaneous distribution of  $x$  given a current value of  $s$ ,  $p(x|s)$ , is a Gaussian centered at  $\bar{x} = s\sigma_{SX}^2/\sigma_{SS}^2$ . This defines the instantaneous gain,  $\tilde{g} \equiv \partial x/\partial s$ , which differs from the macroscopic, static gain  $g \equiv \partial \langle X \rangle / \partial \langle S \rangle$  due to temporal correlations in  $s$  and  $x$ . Shannon's result for the mutual information of a Gaussian channel [4],  $M^{\text{ins}}(s, x) = \frac{1}{2} \ln(1 + P/N)$ , can be obtained by noting that the variance of  $p(x|s)$  is given by  $\sigma_{X|S}^2 = \sigma_{XX}^2 - \sigma_{SX}^4/\sigma_{SS}^2 \equiv N$  and the signal "power"  $P = \tilde{g}^2 \sigma_{SS}^2$ .

*Network motifs*—The three elementary detection motifs shown in Table I [8] illustrate a number of characteristics of the transmission of trajectories. As a simple example of a time-continuous input signal with a non-zero correlation time, we take the dynamics of  $S$  to be a Poissonian birth-and-death process; for large copy numbers, this gives distributions that are approximately Gaussian.

Motif I describes the reversible binding between, for example, a ligand and a receptor, or an enzyme and its substrate. For this motif only we take the signal to be the total density  $s_T = s + x$ . We then find that the frequency-dependent gain  $g^2(\omega)$  scales at high frequencies as  $\omega^{-4}$ , while the frequency-dependent noise  $N(\omega)$  scales as  $\omega^{-2}$ . The gain-to-noise ratio  $g^2(\omega)/N(\omega)$ , which determines how accurately an input signal at frequency  $\omega$  can be transmitted, therefore decays as  $\omega^{-2}$ . Since input signals of biochemical networks are commonly detected via this motif, this result suggests that high-frequency input signals are typically not propagated reliably.

Motif II describes the scenario in which the signaling molecule is deactivated upon detection. An important example is activation of membrane receptors by ligand binding followed by endocytosis. If the input signal obeys Poissonian statistics, the mutual information between instantaneous values of  $S$  and  $X$  is zero— $X$  gives no information about the current value of  $S$ . Indeed, to understand how cells can use this motif to measure concentrations, we have to consider the mutual information between in- and output trajectories. Interestingly, for this motif the noise  $N(\omega)$  vanishes at high frequencies, while the frequency-dependent gain  $g^2(\omega)$  approaches a constant value; the gain-to-noise ratio thus diverges at high frequencies, meaning that this motif can reliably transmit rapidly varying input signals [16].

Motif III is a coarse-grained model for enzymatic reactions or gene activation; the enzyme-substrate or

Scheme	Reaction	$g^2(\omega)$	$N(\omega)$	$ S_{SX}(\omega) ^2/S_{SS}(\omega)S_{XX}(\omega)$
(I)	$S + W \xrightleftharpoons[\mu]{\nu=k_f W} X$	$\left[ \frac{\nu(\mu+\nu+\lambda)}{\omega^2+(\mu+\nu)^2+\nu\lambda} \right]^2$	$\frac{2\nu(S)}{\omega^2+(\mu+\nu)^2+\nu\lambda}$	$\frac{\nu\lambda(\mu+\nu+\lambda)^2}{[\omega^2+(\mu+\nu)^2+\nu\lambda][\omega^2+\lambda(\lambda+\nu)]}$
(II)	$S \xrightarrow{\nu} X \xrightarrow{\mu} \emptyset$	$\frac{\nu^2[\omega^2+(\lambda+\nu)^2]}{4(\lambda+\nu)^2(\omega^2+\mu^2)}$	$\frac{\nu(S)(4\lambda+3\nu)}{2(\lambda+\nu)(\omega^2+\mu^2)}$	$\frac{\nu}{4(\lambda+\nu)}$
(III)	$S \xrightarrow{\nu} S + X, X \xrightarrow{\mu} \emptyset$	$\frac{\nu^2}{\omega^2+\mu^2}$	$\frac{2\nu(S)}{\omega^2+\mu^2}$	$\frac{\nu\lambda}{\omega^2+\lambda(\lambda+\nu)}$

TABLE I: Three elementary detection motifs. The input signal is modeled via  $\emptyset \xrightarrow{k} S$  and  $S \xrightarrow{\lambda} \emptyset$ .

transcription-factor-DNA binding reaction, respectively, has been integrated out. For this motif, which in contrast to the other two obeys the spectral addition rule (Eq. 8),  $g^2(\omega)$  and  $N(\omega)$  have the same functional dependence on  $\omega$ . Hence,  $g^2(\omega)/N(\omega)$  is independent of  $\omega$ , which means that this motif can transmit signals at all frequencies with the same fidelity.

For both motifs II and III the mutual information between trajectories does not depend on the deactivation rate  $\mu$  of the read-out component  $X$ ;  $g^2(\omega)$  and  $N(\omega)$  depend in the same way on  $\mu$ . The information on the input trajectory  $s(t)$  is encoded solely in the statistics of the production events of  $X$ —the decay events occur independently of  $S$  and do not provide new information on  $S$ . These observations may suggest that if an input signal is detected via one of these motifs, the deactivation rate of  $X$  is not important. However, if the information encoded in  $X$  needs to be transmitted to a downstream pathway, then this transmission rate will in general depend on  $\mu$ .

Recently, Endres and Wingreen [12] have argued that detection motif II is superior to motif III in measuring average concentrations. Our analysis shows that motif II can also more reliably transmit information in time-varying signals, due to the more accurate transmission of high frequency components of the input.

*Bacterial chemotaxis*—A classical example of a biological system in which not only the instantaneous value of the input signal is important, but also its history, is the chemotaxis system of *Escherichia coli* [2]. In the *E. coli* chemotaxis network, the messenger CheY is phosphorylated by the kinase CheA and dephosphorylated by the phosphatase CheZ. The kinase activity is rapidly inhibited by receptor-ligand binding, allowing the system to respond to changes in ligand concentration on short time scales, while receptor methylation slowly counteracts the effect of ligand binding on the kinase activity, allowing the system to adapt to changes in ligand concentration on longer time scales. An open question is how this system processes the ligand signal in the presence of noise [13]. Here, we study how reliably the chemotaxis network can transmit information in time-varying input signals.

Recently, Tu *et al.* have shown that a minimal model can accurately describe the response of the chemotaxis system to a wide range of time-varying input signals [14]. In this model it is assumed that receptor-ligand binding

and the kinase response are much faster than CheY<sub>p</sub> dephosphorylation and receptor (de)methylation; it is thus assumed that the kinase activity is in quasi-equilibrium. By linearizing around steady-state, the following model is obtained [14]:

$$a(t) = \alpha m(t) + \beta l(t) \quad (11)$$

$$\frac{dm}{dt} = -\frac{a(t)}{\tau_m} + \eta_m(t) \quad (12)$$

$$\frac{dy}{dt} = \gamma a(t) - \frac{y(t)}{\tau_z} + \eta_y(t). \quad (13)$$

Here,  $a(t)$  and  $m(t)$  are, respectively, the deviations of the fraction of active kinases and the receptor methylation level from their steady-state values;  $l(t)$  and  $y(t)$  are the fractional changes in the ligand and CheY<sub>p</sub> concentrations relative to steady-state levels;  $\tau_m$  and  $\tau_z$  are the time scales for receptor (de)methylation and CheY<sub>p</sub> dephosphorylation, with  $\tau_m > \tau_z$ ;  $\eta_m$  and  $\eta_y$  are Gaussian white-noise sources that are independent of one another, and of the ligand signal:  $\langle \eta(t) \rangle = 0$ ;  $\langle \eta(t)\eta(t') \rangle = \langle \eta^2 \rangle \delta(t-t')$ ;  $\langle \eta_m(t)\eta_y(t') \rangle = \langle \eta(t)l(t') \rangle = 0$ . The statistics of the input signal are described by the power spectrum  $S_{ll}(\omega)$ . This system obeys the spectral addition rule (Eq. 8), and the power spectrum of  $y$  is given by

$$S_{yy}(\omega) = N_{l \rightarrow y}(\omega) + g_{l \rightarrow y}^2(\omega)S_{ll}(\omega), \quad (14)$$

with the noise  $N_{l \rightarrow y}(\omega)$  and the gain  $g_{l \rightarrow y}^2(\omega)$  being intrinsic properties of the chemotaxis network:

$$g_{l \rightarrow y}^2(\omega) = \frac{\beta^2 \gamma^2 \omega^2}{(\omega^2 + \tau_z^{-2})(\omega^2 + \alpha^2/\tau_m^2)}, \quad (15)$$

$$N_{l \rightarrow y}(\omega) = \frac{\alpha^2 \gamma^2 \langle \eta_m^2 \rangle + (\alpha^2/\tau_m^2 + \omega^2) \langle \eta_y^2 \rangle}{(\omega^2 + \tau_z^{-2})(\omega^2 + \alpha^2/\tau_m^2)}. \quad (16)$$

Eq. 15 shows that the gain is small at low frequencies, due to adaptation of the kinase activity via receptor methylation [14] (Fig. 1a). This network is therefore unable to respond to low-frequency variations in the ligand signal. As noted in [14, 15], the gain also decreases at high frequencies, due to the time taken for CheY<sub>p</sub> dephosphorylation by CheZ. However, we see that the noise also decreases with increasing frequency. In fact, at high frequencies the methylation dynamics can be ignored, and the dynamics of CheY<sub>p</sub> are approximately

those of motif III, discussed above. Indeed, at high frequencies  $g_{l \rightarrow y}^2(\omega)/N_{l \rightarrow y}(\omega)$  increases to a constant value, showing that high-frequency components of  $l(t)$  can be reliably transmitted to  $y(t)$ .

These results show how reliably information about the ligand concentration can be encoded in the concentration of the messenger CheY<sub>p</sub>. However, the ultimate response of this system is that of the flagellar motor. Binding of CheY<sub>p</sub> to the motor increases the tendency of the motor to switch to the clockwise state, which causes the bacterium to “tumble” and change direction. Assuming that CheY<sub>p</sub> binding to the motor is fast, and that the motor response can be linearized, the dynamics of the clockwise bias of the motor,  $b(t)$ , is given by

$$\frac{db}{dt} = ky(t) - \frac{b(t)}{\tau_b} + \eta_b(t). \quad (17)$$

Here,  $\tau_b$  is the typical motor switching time and  $\eta_b$  represents Gaussian white noise, uncorrelated from  $\eta_m$  and  $\eta_y$ . Like motif III, this system obeys the spectral addition rule, and the power spectrum of the motor is

$$S_{bb}(\omega) = N_{y \rightarrow b}(\omega) + g_{y \rightarrow b}^2(\omega)S_{yy}(\omega), \quad (18)$$

where  $N_{y \rightarrow b}(\omega) = \langle \eta_b^2 \rangle / (\omega^2 + \tau_b^{-2})$  is the intrinsic noise of the motor, and  $g_{y \rightarrow b}^2(\omega) = k^2 / (\omega^2 + \tau_b^{-2})$  is the frequency-dependent gain of the motor. By inserting  $S_{yy}(\omega)$  of Eq. 14 in Eq. 18, it is seen that the total noise added between the ligand and the motor is given by  $N_{l \rightarrow b}(\omega) = N_{y \rightarrow b}(\omega) + g_{y \rightarrow b}^2(\omega)N_{l \rightarrow y}(\omega)$ , while the gain is given by  $g_{l \rightarrow b}^2(\omega) = g_{l \rightarrow y}^2(\omega)g_{y \rightarrow b}^2(\omega)$ .

Fig. 1b shows that the gain  $g_{l \rightarrow b}^2(\omega)$  is large at frequencies  $\tau_m^{-1} \lesssim \omega \lesssim \tau_z^{-1} \sim \tau_b^{-1}$ , while the noise  $N_{l \rightarrow b}(\omega)$  monotonically decreases with increasing frequency. Importantly, at high frequencies  $\omega \gg \tau_z^{-1}, \tau_b^{-1}$ , the gain  $g_{l \rightarrow b}^2(\omega) \sim \omega^{-4}$  since both  $g_{l \rightarrow y}^2(\omega)$  and  $g_{y \rightarrow b}^2(\omega)$  decrease as  $\omega^{-2}$ , while the noise  $N_{l \rightarrow b}(\omega) \sim \omega^{-2}$  since the dominant contribution to  $N_{l \rightarrow b}(\omega)$  at high frequencies is the intrinsic noise of the motor  $N_{y \rightarrow b}(\omega)$ . As a result, the gain-to-noise ratio,  $g_{l \rightarrow b}^2(\omega)/N_{l \rightarrow b}(\omega)$  scales as  $\omega^{-2}$  for high frequencies. Hence, while high-frequency fluctuations in  $l(t)$  are reliably encoded in the trajectory  $y(t)$ , they are not reliably propagated to the motor. In essence, the high-frequency variations of  $l(t)$  are filtered by the slow dynamics of CheY<sub>p</sub> dephosphorylation and motor switching, and are therefore masked by the inevitable intrinsic noise of motor switching.

The framework presented here allows us to predict the input power spectrum  $S_{ll}(\omega)$  that is most reliably transmitted through the signal transduction pathway (Fig. 2). Our analysis suggests that the *E. coli* chemotaxis network is unable to effectively transmit high- ( $\omega \gg \tau_z^{-1}, \tau_b^{-1}$ ) or

low-frequency ( $\omega \ll \tau_m^{-1}$ ) signals. This prediction could be tested by stimulating *E. coli* cells with input signals of different frequencies [2] and measuring the correlations between the motor bias and the input stimulus.

Finally, we note that the chemotactic signal perceived by an *E. coli* cell depends on its swimming behavior, which is determined by how reliably the chemotaxis network transmits the signal to the motors, which in turn depends on the signal itself (Fig. 1). Further work is needed to study whether nature has optimized this feedback between swimming and signaling.

We thank Martin Howard and Sorin Tănase-Nicola for a critical reading of the manuscript. This work is supported by FOM/NWO.

- 
- [1] M. B. Elowitz, A. J. Levine, E. D. Siggia, and P. S. Swain, *Science* **297**, 1183 (2002).
  - [2] S. M. Block, J. E. Segall, and H. C. Berg, *J. Bacteriol.* **154**, 312 (1983); J. E. Segall, S. M. Block, and H. C. Berg, *Proc. Natl Acad. Sci. USA* **83**, 8987 (1986).
  - [3] C. J. Marshall, *Cell* **80**, 179 (1995).
  - [4] C. E. Shannon, *Bell Syst. Tech. J.* **27**, 379 (1948).
  - [5] P. B. Detwiler, S. Ramanathan, A. Sengupta, and B. I. Shraiman, *Biophys. J.* **79**, 2801 (2000); G. Tkačik, C. G. Callan Jr, and W. Bialek, *Proc. Natl. Acad. Sci. USA* **105**, 12265 (2008); *Phys. Rev. E* **78**, 011910 (2008).
  - [6] E. Ziv, I. Nemenman, and C. H. Wiggins, *PLoS ONE* **2**, e1077 (2007).
  - [7] N. G. Van Kampen, *Stochastic Processes in Physics and Chemistry* (North Holland, Amsterdam, 1992).
  - [8] S. Tănase-Nicola, P. B. Warren, and P. R. ten Wolde, *Phys. Rev. Lett.* **97**, 068102 (2006); arXiv:q-bio/0508027 (2005).
  - [9] P. P. Mitra and J. B. Stark, *Nature (London)* **411**, 1027 (2001).
  - [10] T. Munakata and M. Kamiyabu, *Eur. Phys. J. B* **53**, 239 (2006).
  - [11] R. M. Fano, *Transmission of Information: A Statistical Theory of Communications* (MIT Press, Cambridge MA, 1961).
  - [12] R. G. Endres and N. S. Wingreen, *Proc. Natl Acad. Sci. USA* **105**, 15749 (2008).
  - [13] B. W. Andrews, T.-M. Yi, and P. A. Iglesias, *PLoS Comp. Biol.* **2**, e154 (2006).
  - [14] Y. Tu, T. S. Shimizu, and H. C. Berg, *Proc. Natl Acad. Sci. USA* **105**, 14855 (2008).
  - [15] T. Emonet and P. Cluzel, *Proc. Natl Acad. Sci. USA* **105**, 3304(2008).
  - [16] In fact, the mutual information rate for motif II diverges if the integral in Eq. 7 is taken to infinity. In reality the integral is bounded because a reaction cannot happen infinitely fast, as assumed in the mesoscopic description employed here.

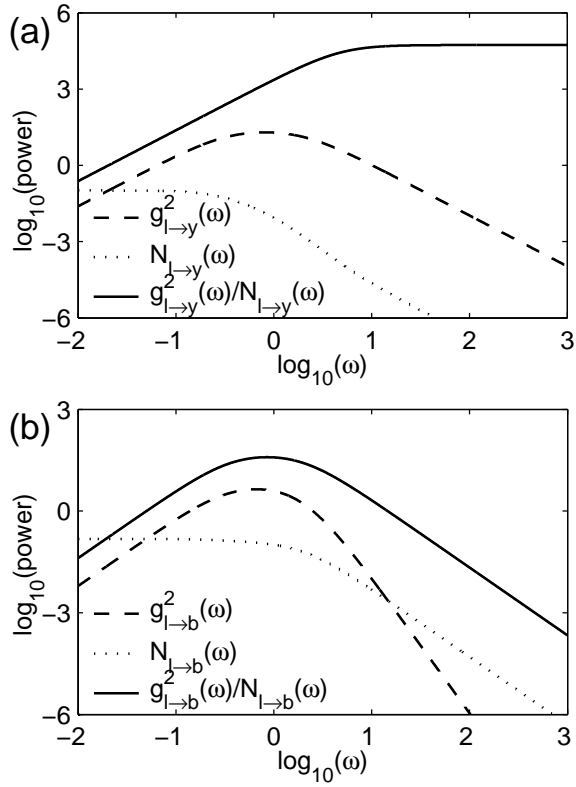


FIG. 1: Information transmission in the *E. coli* chemotaxis network. The network gain  $g^2(\omega)$  (dashed line), noise  $N(\omega)$  (dotted line) and  $g^2(\omega)/N(\omega)$  (full line) are shown between (a) ligand and CheY<sub>p</sub> concentrations, and (b) ligand and motor bias. In Figs 1 and 2 the following parameter values were used, estimated from [14, 15]:  $\alpha = 2.7$ ,  $\beta = -1.3$ ,  $\tau_m = 8\text{s}$ ,  $\langle \eta_m^2 \rangle = 10^{-4}\text{s}^{-1}$ ,  $\gamma = 8\text{s}^{-1}$ ,  $\tau_z = 0.5\text{s}$ ,  $\langle \eta_y^2 \rangle = 0.002\text{s}^{-1}$ ;  $k = 1\text{s}^{-1}$ ,  $\tau_b = 0.5\text{s}$ ,  $\langle \eta_b^2 \rangle = 0.5\text{s}^{-1}$ .

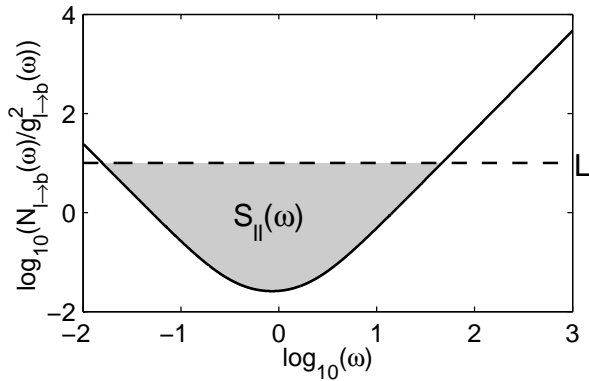


FIG. 2: Water filling approach for the optimal input signal [11]. The optimal power spectrum, subject to a total power constraint  $\bar{S}$ , is given by  $S_{||}(\omega) = L - N_{l \rightarrow b}(\omega)/g_{l \rightarrow b}^2(\omega)$ , with the level  $L$  chosen such that the shaded area matches  $\bar{S}$ .